

This article was downloaded by:

On: 25 January 2011

Access details: *Access Details: Free Access*

Publisher *Taylor & Francis*

Informa Ltd Registered in England and Wales Registered Number: 1072954 Registered office: Mortimer House, 37-41 Mortimer Street, London W1T 3JH, UK



Separation Science and Technology

Publication details, including instructions for authors and subscription information:

<http://www.informaworld.com/smpp/title~content=t713708471>

Interpretation of Transition Metal Sorption Behavior by Oxidized Active Carbons and Other Adsorbents

Vladimir Strelko Jr.^a; Danish J. Malik^a; Michael Streat^a

^a Department of Chemical Engineering, Loughborough University, Loughborough, United Kingdom

Online publication date: 08 July 2010

To cite this Article Strelko Jr., Vladimir , Malik, Danish J. and Streat, Michael(2005) 'Interpretation of Transition Metal Sorption Behavior by Oxidized Active Carbons and Other Adsorbents', *Separation Science and Technology*, 39: 8, 1885 – 1905

To link to this Article: DOI: 10.1081/SS-120030791

URL: <http://dx.doi.org/10.1081/SS-120030791>

PLEASE SCROLL DOWN FOR ARTICLE

Full terms and conditions of use: <http://www.informaworld.com/terms-and-conditions-of-access.pdf>

This article may be used for research, teaching and private study purposes. Any substantial or systematic reproduction, re-distribution, re-selling, loan or sub-licensing, systematic supply or distribution in any form to anyone is expressly forbidden.

The publisher does not give any warranty express or implied or make any representation that the contents will be complete or accurate or up to date. The accuracy of any instructions, formulae and drug doses should be independently verified with primary sources. The publisher shall not be liable for any loss, actions, claims, proceedings, demand or costs or damages whatsoever or howsoever caused arising directly or indirectly in connection with or arising out of the use of this material.

Interpretation of Transition Metal Sorption Behavior by Oxidized Active Carbons and Other Adsorbents

Vladimir Strelko Jr., Danish J. Malik,* and Michael Streat

Department of Chemical Engineering, Loughborough University,
Loughborough, United Kingdom

ABSTRACT

Several active carbons derived from different precursors and oxidized by different techniques have been characterized by N_2 porosimetry and various titration methods. The adsorption of Cu^{2+} , Ni^{2+} , Co^{2+} , Zn^{2+} and Mn^{2+} from aqueous solutions was studied using these carbons and carboxylic resin Purolite C104. The affinity series $Mn^{2+} < Co^{2+} < Ni^{2+} < Cu^{2+} > Zn^{2+}$ established in adsorption experiments coincides with the Irving–Williams order and is independent of the method and extent of adsorbent oxidation, carbon precursor, porous structure, and type of adsorbent. Enhanced selectivity of adsorbents towards Cu^{2+} is related to the electronic structure of this ion.

Key Words: Oxidized carbon; Transition metal sorption; Selectivity; The Irving–Williams series; Surface oxygen complexes.

*Correspondence: Danish J. Malik, Department of Chemical Engineering, Loughborough University, Loughborough LE11 3TU, United Kingdom; Fax: +44-1509-223923; E-mail: d.j.malik@lboro.ac.uk.

INTRODUCTION

A review of previous publications shows certain scientific interest in the adsorption of heavy metal ions from aqueous solutions by carbonaceous materials.^[1-5] It is widely accepted that surface acidic functional groups are responsible for metal ion binding.^[2,4,6] Chemical oxidation is a commonly used method to introduce these functional groups on the surface of carbons.^[6] Sorptive capacity and selectivity of oxidized carbon vary for different metal ions and higher valency metal ions are usually preferred to those with lower valency.^[7,8] It is also observed that metal sorptive selectivity of carbons differs even within a series of metals with the same valency. Thus, it was shown by many researchers that among the double-valency metals, Cu^{2+} is generally the most preferred ion.^[1,2,5,7,8] However, the reasons for the higher affinity of oxidized carbons towards this particular metal ion have not been clearly identified. Improved conception of this phenomenon is essential for the development of novel separation processes. An excellent review on the ion exchange properties of carbon materials has been published by Radovic et al.^[9]

In the present work, a series of oxidized carbons were applied to the adsorption of d-block metal ions such as Cu^{2+} , Ni^{2+} , Co^{2+} , Zn^{2+} , and Mn^{2+} from aqueous solutions. The physicochemical properties of the adsorbents were compared using N_2 porosimetry, Boehm's titration, and pH titration. An attempt was made to identify the parameters responsible for enhanced selectivity of oxidized carbon towards Cu^{2+} .

EXPERIMENTAL

Materials

Active carbons derived from agricultural by-products (apricot stones; designated as KAU) and one made from polystyrene cross-linked with divinylbenzene (DVB) (designated as CKC) were precursors from which oxidized active carbons were prepared and evaluated for the current study [the materials were supplied by the Institute of Sorption and Problems of Endoecology (ISPE), NAS of Ukraine].

The KAU-carbons were prepared as follows: (1) treatment of crushed fruit stones with a hot solution of strong alkali; (2) washing with water to bring the pH of solution down to 10; (3) treatment of crushed fruit stones with hot hydrochloric acid; (4) washing with water to bring pH of solution up to 4; (5) carbonization at 350–700°C; and (6) activation with steam at 800–850°C.



Preparation of the CKC-carbon was carried out as follows: (1) the copolymer was swollen in monochlorodimethylester for 24 hr; (2) chemical carbonization in sulfuric acid at 130–150°C was carried out for 6–9 hr; (3) carbonization at 380–420°C for 4 hr with steam; (4) preactivation treatment at 700°C for 4 hr in a nitrogen atmosphere; and (5) finally, the material was activated at 850°C for 3 hr using steam as the activation agent.

Carbonaceous materials were modified by oxidation using either nitric acid, hot dry air, or electrochemical oxidation techniques. The carbon oxidation methodologies can be found elsewhere.^[10–12] Table 1 presents the conditions of oxidation of the materials used in the current study.

A commercial unoxidized activated carbon supplied by Chemviron (designated F400) was also studied. Oxidation of the F400 carbon [designated F400(ox)] was performed at 90°C using 20% (v/v) nitric acid for 15 hr. Carbon to acid ratio was 1:3 (v/v). The oxidizing agent was replaced halfway through the oxidation with fresh 20% (v/v) nitric acid. By-products of carbon oxidation (humic compounds) were removed using distilled water followed by treatment with 1–3% (wt/wt) sodium hydroxide, and finally with distilled water until the solution pH was reduced down to pH 9–10. Protonation of the oxidized carbon was carried out by treatment with 2–5% (wt/wt) hydrochloric acid followed by a final wash with distilled water. The washed material was dried at 105°C and then stored in an airtight container.

Table 1. List of adsorbents and conditions of their synthesis.

Sorbent	Precursor	Oxidation conditions
F400	Coal	Unoxidized
F400(ox)	Coal	15 h in hot HNO ₃ (8 N), at 90–95°C ^a
KAUini	Apricot stones	Unoxidized
KAU-1.8	Apricot stones	5 hr in air at 450°C
KAU-2.9	Apricot stones	15 hr in hot HNO ₃ (8 N), at 90–95°C ^a
KAU-1-25	Apricot stones	Electrochemically for 1 hr at 25°C, current 988 mA ^b
KAU-5-25	Apricot stones	Electrochemically for 3 hr at 25°C, current 988 mA ^b
CKC	Styrene–DVB	15 hr in hot HNO ₃ (8 N), at 90–95°C ^a
CKC-3-25	Styrene–DVB	Electrochemically for 3 hr at 25°C, current 988 mA ^b

^aCarbon : acid ratio is 1:3 (v/v).

^bElectrochemical oxidation of carbons (as anode in an electrochemical cell with a platinum cathode) was carried out by applying a current (988 mA) for 1, 3, or 5 hr in the presence of 1 M KCl.



A carboxylate ion exchange resin, Purolite C104 (capacity $\sim 10 \text{ mmol g}^{-1}$), was used as a reference material.

Surface Area and Pore Size Distribution

Surface area and pore size distribution of all carbons were determined from nitrogen adsorption–desorption isotherms at 77 K measured by means of a Micromeritics ASAP 2010 surface area analyzer. Carbon samples were outgassed for a minimum of 24 hr at 120°C on the degas port of the analyzer. The data was modeled using the DFT (Density Functional Theory) method.^[13]

Boehm's Titrations

The relative concentrations of different surface functional groups in oxidized carbons were determined by Boehm's method.^[14] Amounts of dry carbon, 0.2 g, were weighed into 50 mL conical flasks prior to the addition of 20 mL of base of varying strength, e.g., 0.1 N solution of sodium hydrogen carbonate, sodium carbonate, sodium hydroxide, and sodium ethoxide. Carbon samples were agitated for 72 hr at room temperature. The supernatant solutions were separated using 0.45 μm PTFE syringe top filters. Aliquots, 5 mL, were then titrated with 0.1 N hydrochloric acid using methyl-red as the indicator (pK 5, pH range 4.8–6). High purity water with the resistance greater than 15 M Ω was used in all titration experiments.

pH Titrations

pH titrations of adsorbents were carried out using the method described by Helfferich.^[15] Typically, a number of samples (75 mg each) of sorbent (particle size less than 45 μm) were weighed into separate flasks. A set of samples was prepared with successively larger amounts of 0.1 M NaOH or HCl added to the different samples using a micropipette. Then, 10 mL of 0.1 M NaCl solution was added to each flask to keep a high background electrolyte concentration. A total batch volume of 15 mL was made up by adding distilled water to maintain the solution volume to sorbent weight ratio constant. A blank experiment with no carbon was also performed. The batches were equilibrated for 48 hr after which the pH of the supernatant solution was recorded using a Mettler-Toledo 340 pH meter. Proton release/uptake values as a function of equilibrium pH were obtained as follows: a pH vs. (NaOH added) curve was plotted for the batch samples before adding



the carbon samples to each flask; after equilibration, a new pH vs. (NaOH added) curve was obtained. At a given pH, the difference between the two curves provided values of proton release vs. uptake.

pH titration data were fitted using the method described by Seki and Suzuki^[16] that also allowed extracting acid-dissociation constants for the acidic sites on the cation-exchanger between pH \sim 2 and \sim 10.5. The acid-dissociation reactions for surface groups can be written as:



The acid-dissociation constant K for a particular type of functional groups is defined as:

$$K_{1,2} = \frac{\alpha[\text{H}^+]}{1 - \alpha} \quad (3)$$

where α is the degree of dissociation of functional groups. The number of deprotonated acidic groups on carbon (dry wt. basis, g), X_o , can be expressed as:

$$X_o = N\alpha = \frac{NK_{1,2}}{K + [\text{H}^+]} \quad (4)$$

where N represents the number of acidic groups on carbon. Equation (4) may be fitted to titration data (deprotonated acidic groups, mmol g^{-1} vs. equilibrium pH) to extract values for the two unknown parameters, N and $K_{1,2}$.

Transition Metal Sorption

Sorption of copper(II), nickel(II), cobalt(II), zinc(II), and manganese(II) from nitrate solutions was studied in batch experiments (to obtain metal ion sorption data at pH 4.8 and selectivity coefficient values at pH 4.2) and small columns (to obtain maximum metal uptake data at pH 4.8).

Equilibrium metal ion sorption isotherms were obtained in the following way. Fifty milligrams of granular carbon particles were accurately weighed out into 250 mL conical flasks. Metal nitrate feed solutions of 200 mL (concentration range: 0.06–0.36 mmol L^{-1}) were added to each flask. The flasks were agitated for 48 hr using a Stuart Scientific flask shaker at $22^\circ\text{C} \pm 2^\circ\text{C}$. The batch samples were maintained at pH 4.8 by addition of a small amount of sodium hydroxide. After equilibration small aliquots of supernatant solutions were separated and analyzed for metal content using a Varian



SpectrAA-200 atomic absorption spectrophotometer (AAS) in flame mode with an air–acetylene flame.

The maximum metal ion uptake capacity of the oxidized material for the metal series was determined by passing a metal-bearing solution (pH of the solution was fixed at pH 4.8) through a mini-column packed with a small amount of carbon (~100 mg). After saturation, the adsorbent samples were washed with distilled water, dried, and then digested in a mixture of concentrated perchloric and nitric acids (2 : 1 v/v) to determine the metal sorptive capacity of carbon. The metal concentrations were determined by atomic absorption spectrometry.

Calculation of Metal-Complex Stability Data

Complexation reaction between a cation and protonated form (functional groups) of oxidized carbon can be written in the following manner:



where n is the number of functional groups (ligands), interacting with one metal ion, and z is a charge of a complex-forming ion.

Equilibrium constant of such a reaction is described by the following expression:

$$K_{\text{eq}} = \frac{[\text{R}_n\text{Me}^{z-n}][\text{H}^+]^n}{[\text{Me}^{z+}][\text{RH}]^n} \quad (6)$$

where $[\text{RH}]$ is the overall concentration of functional groups on the surface, $[\text{R}^-]$ is the amount of dissociated functional groups, $[\text{R}_n\text{Me}^{z-n}]$ is the amount of complexed ions and $[\text{Me}^z]$ represents the concentration of uncomplexed ions.

Decomposition of the surface metal–carbon complex is written as in Eq. (7)



And the overall complex stability constant can be expressed as in Eq. (8)

$$K_{\text{st}} = \frac{[\text{Me}^{z+}][\text{R}^-]^n}{[\text{R}_n\text{Me}^{z-n}]} \quad (8)$$



The dissociation of protonogenic groups will also influence the total equilibrium and is defined by the dissociation constant expressed in Eq. (9).

$$K_{\text{dis}} = \frac{[\text{H}^+][\text{R}^-]}{[\text{HR}]} \quad (9)$$

Taking into account the processes described above, surface complex stability constant should be written as in Eq. (10).

$$K_{\text{st}} = \frac{K_{\text{dis}}^n}{K_{\text{eq}}} \quad (10)$$

In order to determine the equilibrium constant of surface complexation according to Eq. (10), it is necessary to know an average number (n) of ligands (functional groups) interacting with one metal ion. Assuming that the carbon surface complexes are of a chelate type and z is the number of functional groups reacting with each metal ion, then, the equilibrium complexation constant can be equalized to the exchange constant as in Eq. (11).

$$K_{\text{Me}^{z+}-\text{H}^+} = \frac{[\text{R}_z\text{Me}][\text{H}^+]}{[\text{RH}]^z[\text{Me}^{z+}]} \quad (11)$$

In this case, the stability constant for Me^{z+} -oxidized carbon can be expressed as in Eq. (12).

$$K_{\text{st}} = \frac{K_{\text{dis}}^z}{K_{\text{ex}}} \quad (12)$$

Since an oxidized carbon may be considered a polyfunctional adsorbent, it can be assumed that method of calculation of stability constants K_{st} (as described above) would be relatively correct provided that K_{dis} and K_{ex} are determined at the same pH and surface saturation degrees.

RESULTS AND DISCUSSION

Surface Area and Pore Size Distribution

The microporous nature of the carbons evaluated during the current study is demonstrated in Figs. 1–3. In general, oxidation slightly reduces the micro-pore volume and hence the surface area of the adsorbents (refer to Table 2). Oxidation of carbon samples results in a slight enhancement of mesopore volume.

The reduction in surface area and pore volume of carbon after oxidation, also observed by some researchers,^[17,18] may be related to several



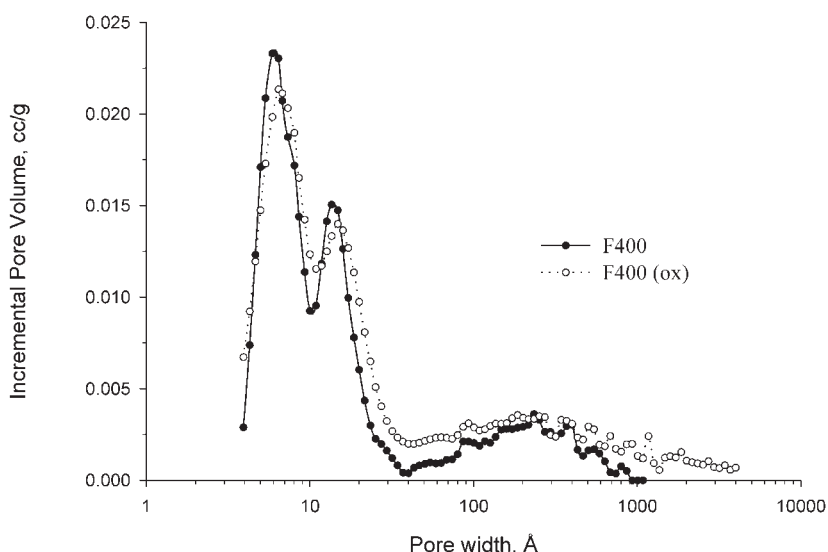


Figure 1. Pore size distribution data for F400 and F400(ox) carbons.

factors such as pore entrance blockage by oxygenated surface functional groups and large molecules of residual humic-type compounds, electrostatic repulsion of surface probe molecules (nitrogen), and erosion of carbon by nitric acid.

Oxidized and unoxidized carbon samples possess a significant amount of micropores (pore size less than 20 Å) and mesopores in the range 20–800 Å. The data also provides some evidence supporting that there is a widening of pores after the oxidation treatment (see Fig. 3 for the CKC-3-25 carbon). In the case of the F400(ox) sample, there is some enhancement in the pore volume attributed to mesopores (40–200 Å) and a slight reduction in pore volume attributed to micropores. This may predominantly be related to the widening and, hence, transition of micropores into mesopores following the highly corrosive nitric acid oxidation process.

The apparent bimodal distribution of pores in the microporous region (e.g., for F400 and CKC samples) is caused by deficiencies of the DFT model. This theory is not able to accurately model pores in the 8–10 Å range due to a theoretical discontinuity. Nevertheless, the pore size determination below 8 Å is considered accurate.^[13,19] On the other hand, the well-known and commonly used BET method^[20] may not be applied for the micropore region of active carbons. This is due to the fact that nitrogen adsorption is much stronger in micropores than in meso/macropores and therefore may not be described by the theory of capillary condensation.



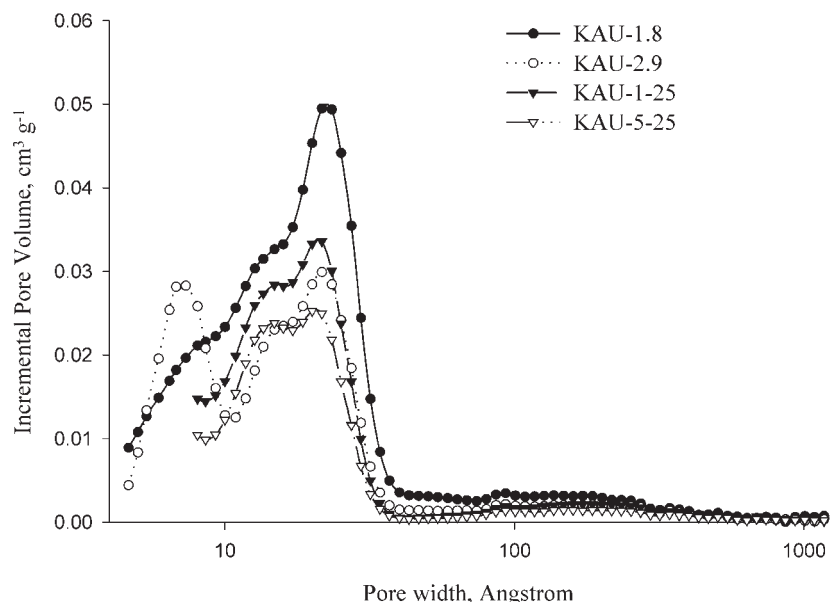


Figure 2. Pore size distribution data for KAU carbon series.

The determination of pore size distribution in the micropore region (defined as 20 Å and below) is less certain. Methods based on the potential theory of Dubinin, *t*- or α -plots or the MP method, are widely used.^[20,21] Pore size distributions above 20 Å are usually assessed using the method of Barrett, Joyner, and Halenda (BJH) and other methods.^[20,22] Unlike these methods, the DFT method is applicable for the entire range of pore sizes accessible by the adsorptive molecule (nitrogen) that makes this technique very attractive.

Boehm's Titration

The distributions of surface functional groups at the surface of the adsorbent materials are presented in Table 3. The Boehm's titration results show that the carbonaceous adsorbents possess weak acidic surface functionalities in a form of noncarbonyl (i.e., carboxylic, lactonic and phenolic groups) and carbonyl groups. The overall exchange capacity of the F400 carbon drastically increases after nitric acid oxidation (~13-fold increase). The increase in the individual types of functional groups after oxidation does not occur in



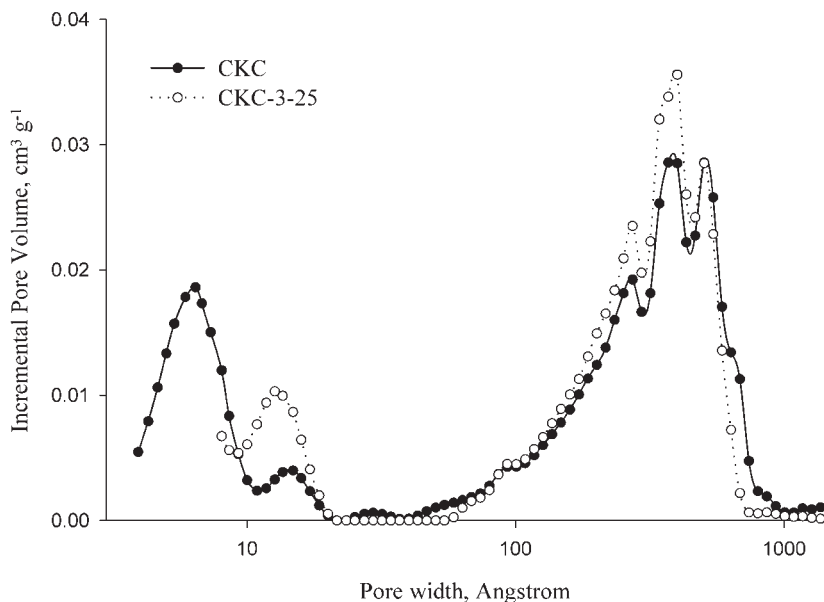


Figure 3. Pore size distribution data for CKC and CKC-3-25 carbons.

equal proportions. These changes are reflected in the distribution of surface groups in the oxidized sample. Thus, the groups neutralized by NaHCO_3 (carboxylic groups) represent about 38% of the total number of acidic non-carbonyl groups for untreated active carbon F400, whilst after oxidation carboxylic groups represent nearly 45% of the oxidized F400 sample.

Table 2. Surface area and pore volume results.

Sorbent	DFT_{SA} ($\text{m}^2 \text{g}^{-1}$)	S_{Mic} ($\text{m}^2 \text{g}^{-1}$)	S_{Mes} ($\text{m}^2 \text{g}^{-1}$)	DFT_{PV} ($\text{cm}^3 \text{g}^{-1}$)	V_{Mic} ($\text{cm}^3 \text{g}^{-1}$)	V_{Mes} ($\text{cm}^3 \text{g}^{-1}$)	S_{BET} ($\text{m}^2 \text{g}^{-1}$)
F400	945	905	40	0.34	0.16	0.18	930
F400(ox)	850	800	50	0.27	0.06	0.21	1008
KAUini	1190	n.a.	n.a.	0.75	n.a.	n.a.	1823
KAU-1.8	1150	970	180	0.83	0.55	0.28	1870
KAU-2.9	949	810	139	0.58	0.37	0.21	1369
KAU-1-25	n.a.	—	—	n.a.	—	—	1587
KAU-5-25	n.a.	—	—	n.a.	—	—	1280
CKC	569	n.a.	n.a.	0.63	n.a.	n.a.	546
CKC-3-25	n.a.	—	—	n.a.	—	—	679

Note: n.a., data unavailable.



Table 3. Concentration and distribution of surface functional groups in carbons.

Carbon	Carboxylic groups (meq g ⁻¹)	Lactones (meq g ⁻¹)	Phenolic groups (meq g ⁻¹)	Total (noncarbonyl meq g ⁻¹)	Carbonyl groups (meq g ⁻¹)	Total capacity (meq g ⁻¹)
F400	0.047	0.073	0.003	0.123	0.235	0.358
%	38.21	59.35	2.44	100		
F400(ox)	0.719	0.439	0.427	1.586	1.356	2.941
%	45.33	27.68	26.92	100		
KAUini	0.078	0	0.370	0.448	0.628	1.076
%	17.41	0	82.59	100		
KAU-1.8	0.540	0.560	0.680	1.779	0.664	2.443
%	30.35	31.48	38.22	100		
KAU-2.9	1.430	0.650	0.795	2.875	2.531	5.405
%	49.74	22.61	27.65	100		
KAU-1-25	0.580	0.320	0.380	1.280	1.170	2.450
%	45.30	25.00	29.70	100		
KAU-5-25	1.580	0.665	0.830	3.075	1.390	4.465
%	51.40	21.60	27.00	100		
CKC	1.149	0.585	0.462	2.160	1.056	3.216
%	53.19	27.08	21.39	100		
CKC-3-25	1.366	0.479	0.540	2.385	1.615	4.000
%	57.27	20.09	22.64	100		

Note: % in comparison to the total noncarbonyl capacity.

Contrary to the modified carbon, unoxidized F400 possesses a greater proportion of relatively weaker functional groups (lactones); the actual concentrations are much smaller.

The total exchange capacity of unoxidized F400 is very low when compared to the oxidized modification. It is also significantly lower than the figure of 1.05 meq g⁻¹ presented by Mazet et al.^[23] The difference may be due to the variation in chemical composition of the powdered F400 active carbon titrated by these researchers. Their material may have been exposed to an oxidizing atmosphere (air) for a longer period than our carbon sample. This would obviously result in a greater amount of acidic groups attached to the carbon surface.

The concentration of strongly acidic groups substantially increases after oxidation. (Note: In this paper, carboxylic groups are considered to be strongly acidic. In comparison with other oxygen-containing groups on the carbon surface e.g., phenolic, lactonic, quinone, etc., carboxyl groups have the lowest pKa values.) Thus, the number of strongly acidic groups neutralized by NaHCO₃ (carboxylic groups) corresponds to 1.43 meq g⁻¹, i.e., almost 50% of the total (noncarbonyl groups) for KAU-2.9.



The total acidity can be increased by a factor of five compared to that of the original KAUini for carbons oxidized with nitric acid. The increase in total acid capacity is about two times that of the starting material for the air-oxidized carbon KAU-1.8. Oxidation of carbon KAUini using the nitric acid oxidation or the electrochemical oxidation technique creates a greater quantity of relatively strong carboxylic surface groups. In general, thermal treatment of carbons in an oxidizing atmosphere leads to a smaller increase in the total acidity of the final material in comparison with low temperature treatments, e.g., nitric acid and the electrochemical technique.

pH Titration

Proton-binding pH-titration curves for the unoxidized carbon sample F400 and the oxidized carbon F400(ox) are shown in Fig. 4. Basic properties are dominant for untreated F400 up to pH 8. Thus, F400 may be described as an H-type carbon.^[24] This is contrary to the acid–base behavior of oxidized F400 that exhibits acidic properties above pH 2 and may be categorized as an L-type carbon. The absolute value of proton binding (ordinate) from the

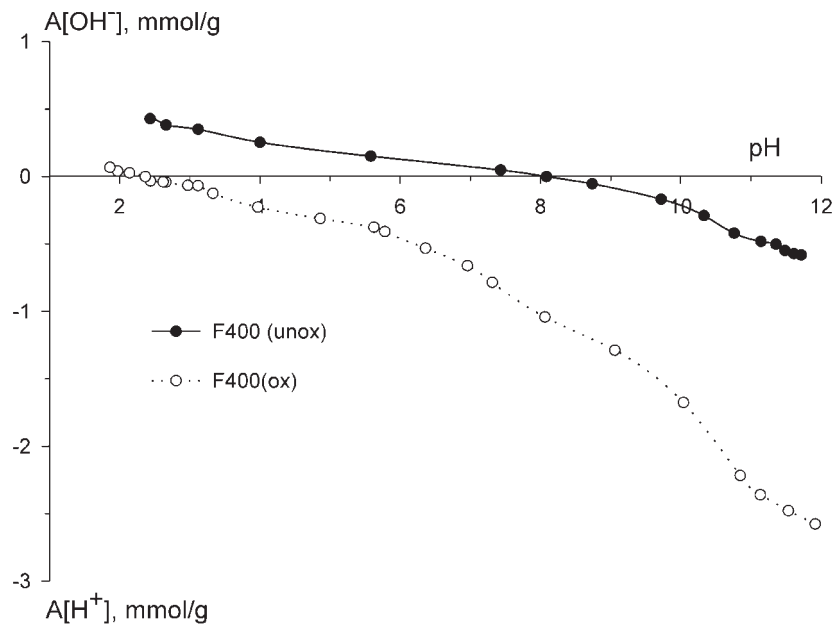


Figure 4. Proton-binding curves for F400 and F400(ox).



titration curve of the unoxidized F400 carbon suggests very low cation-exchange capacity. However, this carbon, being of a more basic nature, displays much higher anion-exchange capacity. Titration of both samples with 0.1 N hydrochloric acid yielded the capacities of approx. 0.5 and 0.16 mmol g⁻¹ for the unoxidized and oxidized carbons, respectively.

The titration curves for all the oxidized samples [only F400(ox) is shown as a representative curve] were smooth and did not display distinctive inflection points indicating the polyfunctional nature of the adsorbent surface. The pH titration curves of the oxidized carbons displayed a shallow descent in the pH range between 2 and 4, which is due to suppressed dissociation of surface functional groups. However, the gradient of the curve progressively increased as the pH increased. This was particularly notable between pHs \sim 4 and 10. As the solution pH progressively increased, weaker functional groups (lactones, phenols, etc.) began to dissociate, thereby contributing to the total exchange capacity of the material.

Dissociation constants of acidic functional groups in the unoxidized and the oxidized carbons exhibit greatly different values that vary between 10⁻² and 10⁻¹¹ (Table 4). This again confirms the polyfunctional nature of carbonaceous materials.

Point of Zero Charge and Isoelectric Point

The crossover point with the pH axis on the differential titration curves is the point where anion and cation exchange processes are at equilibrium.

Table 4. Electrochemical properties and dissociation constants of the adsorbents.

Sorbent	pH _{IEP} ^a	pH _{PZC}	pK _a 1	pK _a 2	pK _a 3	pK _a 4
F400	5.8	8.1	—	—	9.8	10.33
F400(ox)	1.3	2.5	3.6	5.9	7.2	9.7
KAUini	2.5	9.9	—	—	10.0	—
KAU-1.8	1.7	3	3.6	7	9.2	10.8
KAU-2.9	1.1	2.1	3.6	6.5	8.5	10.0
KAU-1-25	1.5	2.6	3.8	5.1	6.6	7.68
KAU-5-25	1.3	2.0	2.6	3.45	5.5	7.2
CKC	1.1	2.1	2.8	5.6	6.9	9.8
CKC-3-25	1.1	2.1	2.4	3.9	7.15	8.5
C104	2	3	5.3	—	—	—

^aIEP values were obtained by extrapolation.



This point is considered to be a point of zero charge (PZC). At solution pH values less than the PZC, the surface has a net negative charge, while at pH values greater than the PZC, the surface has a net positive charge. As the degree of carbon oxidation increases, the crossover point occurs at lower pH values. Thus, the crossover point for untreated F400 is located at pH \sim 8.1, whereas that for the oxidized F400 is at pH \sim 2.5.

Oxidation of the carbon surface is a diffusion-dependent process due to the highly porous nature of the carbonaceous materials. Oxidation occurs faster on the external surface than on the internal surface. Alkalimetric titration is a process that involves the transfer of protons and hydroxyl-ions between the bulk phase (i.e., solution) and the surface of the carbon (micropores and mesopores). The PZC value generated from these experiments, therefore, is representative of the net total (outside, i.e., circumferential and internal) surface charge of the particles. Electrophoretic mobility measurement detects the potential at the shear plane of double electric layer that is adjacent to the external surface.^[3,25] Hence, the isoelectric point (IEP) values determined by this method are only representative of the external surface charges of carbon particles in aqueous solutions. Consequently, the difference between PZC and IEP can be interpreted as a measure of surface charge distribution of porous carbon solids.^[25] Greater $\text{pH}_{\text{PZC}} - \text{pH}_{\text{IEP}}$ values indicate a more negatively charged external than internal particle surfaces. Lower values suggest a more homogeneous distribution of the surface charges. Table 4 presents the PZC and IEP values for the carbon samples studied.

A greater difference between PZC and IEP values was observed for the unoxidized samples F400 and KAUini. Since these carbons were not kept in an inert atmosphere, aging (slow oxidation by air) of the samples may have occurred. The high values of PZC for F400 and KAUini indicate that the internal surface still preserves its basic character. The oxidation of the surface preferentially occurs on the external surface and this is indicated by the lower IEP values for these carbons. The difference between PZC and IEP values decreases along with the individual recorded values for the oxidized materials. The close values of PZC and IEP for KAU-2.9, KAU-5-25, and CKC-3-25 indicate that the oxidation treatments affect the entire surface, i.e., internal and external surfaces to a similar extent, i.e., concentrations of functional groups on the external and internal surfaces are quite similar (Table 4).

Metal Sorption Studies

Modification of carbons results in a small reduction of surface area (Table 2). This is attributed to pore entrance blockage by oxygenated surface

functional groups and large molecules of residual humic-type compounds, electrostatic repulsion of surface probe molecules (N_2), and erosion of carbon by oxidation treatment. Oxidation of carbons strongly influences their surface chemical properties. This is confirmed by the results of Boehm's titration (Table 3). It can be seen that the distribution of surface acidic functional groups depends on the type and extent of treatment. The proportion of relatively weaker groups (i.e., lactonic and phenolic) is characteristic of low degrees of surface oxidation, e.g., for KAU-1.8. In contrast, acid and electrochemical oxidation treatments produce a higher proportion of carboxylic groups. Sodium hydroxide titration data (represented as "total noncarbonyl") shows that oxidation treatments have produced adsorbents with considerably varying total exchange capacities.

The diversity of acid–base surface properties of adsorbents is also reported in Table 3. With the exception of the unoxidized carbon F400, all carbons evaluated in the current study exhibit a negative surface charge over the pH range studied ($< pH 5$). As inferred from the IEP and PZC values, the extent of surface charge varies with the degree of surface oxidation. The surface of carbon (oxidized to a higher degree) displays a greater surface negative charge. On the basis of the Boehm's titration results, dissociation of surface functional groups may be characterized by four discrete dissociation constants (pK_a). Surface oxidation generates a distribution of surface functional groups. The position of these different surface groups in close proximity to one another may influence their acidity and, hence, impact on the mechanism by which hydrated metal ions are sequestered from solution. For example, the acidity increases by more than an order of magnitude from benzoic to *m*-phthalic and salicylic acids. The surface carboxyl groups of oxidized carbons exhibit even lower dissociation constants. This may be related to the fact that the surface groups are connected to a π -conjugated condensed system of graphite-like planes. The number of the conjugated benzene rings and the positioning of the groups will also influence their acidity. For example, carboxylic acids derived from naphthalene and anthracene possess different dissociation constants depending on the location of the carboxylic functional group on the aromatic ring.^[26]

The results of metal sorption have revealed that the uptake and selectivity towards Cu^{2+} ions exhibited by the adsorbents is greater than that for Ni^{2+} , Co^{2+} , Zn^{2+} , and Mn^{2+} (refer to Fig. 5). Variations in the uptake of the other metal ions were also detected, e.g., Co^{2+} and Zn^{2+} were less preferred than Ni^{2+} and Mn^{2+} was the least favored ion. Figure 5 clearly indicates that the complex stability/selectivity trend remains independent of the method and extent of adsorbent oxidation (compare air, acid, and electrochemical oxidation), the type of carbon precursor (compare coal, apricot stones, and polymer derived carbons), the porous structure, and the type of adsorbent

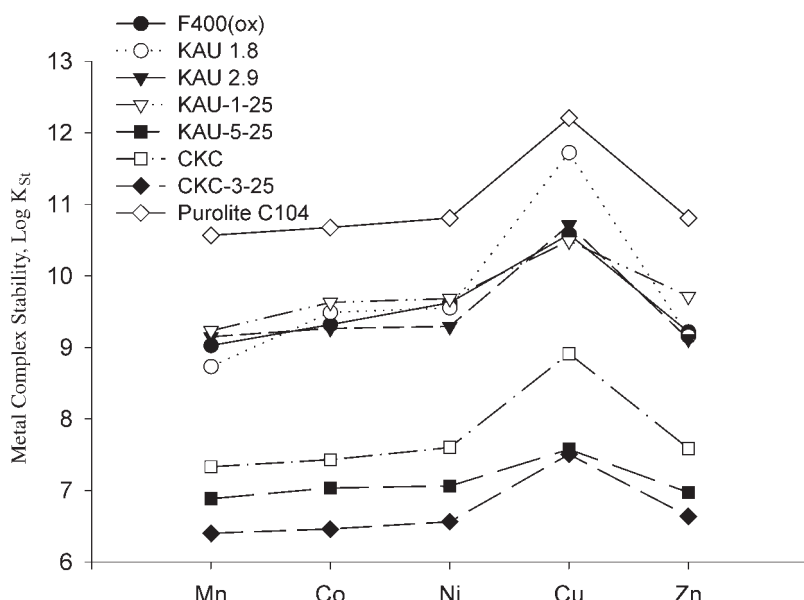


Figure 5. Stability constants of Me^{2+} –adsorbent surface complexes.

(compare carbons vs. the carboxylic cation exchanger) for all adsorptive materials investigated. Correlations of metal uptake as a function of individual groups, e.g., carboxylic, or lactonic, or sum total of noncarbonyl groups did not show a linear trend. Based on the metal sorption data discussed above, the relative sorption affinity of metal ions can be described as follows (the arrangement of metals in the sequence is the same as in the Periodic table): $\text{Mn}^{2+} < \text{Co}^{2+} < \text{Ni}^{2+} < \text{Cu}^{2+} > \text{Zn}^{2+}$.

The highest preference of all adsorbents for Cu^{2+} and the position of metals in the affinity series coincide with the order described by the Irving–Williams series.^[27] This series relates the electronic structure of the central metal ion with the stabilities of its complexes. The order of metals in the Irving–Williams series follows the ionic radii of transition metal ions and is relatively insensitive to the choice and the number of ligands involved.

The variation in stability of transition metal complexes may be related to several factors. The metal–ligand interactions intensify in magnitude and the stability of the complex increases with the reduction of metal ionic radius.^[28] The decline at the end of the stability series is related to the increasing ionic radii. The ligand-field stabilization energy (LFSE), which is related to the electronic configuration of the metal ion, is the other factor responsible for the variable complex stability.^[28,29] As a rule, the greater LFSE is associated



with the more stable complex. Consideration in terms of the ionic radius or the LFSE shows that both factors predict that the maximum stabilities should be associated with complexes of Ni^{2+} rather than those of Cu^{2+} . This anomaly is a consequence of the stabilizing influence of the Jahn–Teller distortion,^[29] which results in stronger binding of the four ligands in the plane of the tetragonally distorted Cu^{2+} complex. The typical pattern of Jahn–Teller distortions, observed in Cu^{2+} complexes, involves the formation of four shorter bonds and two transbonds that are considerably longer than the remaining four (tetragonal distortion). The reason for the Jahn–Teller distortion is because the ninth electron in copper is placed into a set of the e_g orbitals in such a way as to produce an asymmetric electron population (i.e., two in one orbital and one in the other). This distortion is possible for any electronic configuration with asymmetry of this kind. The electron population of the e_g orbitals is symmetric in Ni^{2+} (i.e., one electron in each orbital) and, therefore, this ion does not exhibit any distortion.

Many Cu^{2+} complexes are known to have either four short bonds and two long bonds or two short and four long bonds. The outcome is that the Jahn–Teller distortion of Cu^{2+} compounds yields shorter and stronger metal–ligand bonds (stronger complexes) than might be expected on the basis of the isotropic “ionic radius” of Cu^{2+} .

The correlation between low molecular weight metal complexes with carboxylic acids, hydroxy-acids, and other compounds (as described in the Irving–Williams series) with Me^{z+} –O–C bonds can only be remote to the surface complexes between Me^{z+} and adsorbent. However, there is good correlation between the stability of such complexes^[30] and the metal sorption by adsorptive materials studied (refer to Figs. 5 and 6).

The formation of metal surface complexes on the oxidized carbon involving cooperative action seems quite likely. Approximate calculation of oxygenated functional group density per unit area for F400(ox) yields a value of 0.02 functional groups per squared angstrom. Given that the oxidized carbons evaluated in the present study possess a large proportion of pores in the region of 10–20 Å and the diameter of the hydrated metal ions is approximately 8 Å,^[31] it is reasonable to assume a cooperative binding mechanism (see Fig. 7).

CONCLUSIONS

In summary, the results of metal sorption show that all adsorbents exhibit an ability to remove metal ions from aqueous solutions with varying affinity in the order $\text{Mn}^{2+} < \text{Co}^{2+} < \text{Ni}^{2+} < \text{Cu}^{2+} > \text{Zn}^{2+}$. This coincides with the general stability sequence of metal complexes (the Irving–Williams series).

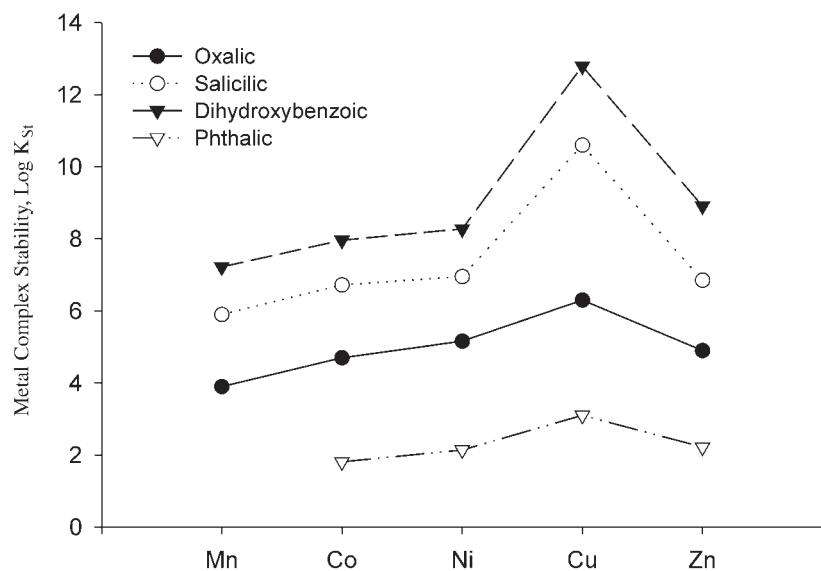


Figure 6. Stability constants of Me^{2+} –carboxylic acid complexes. *Source:* Adapted from Ref. [29].

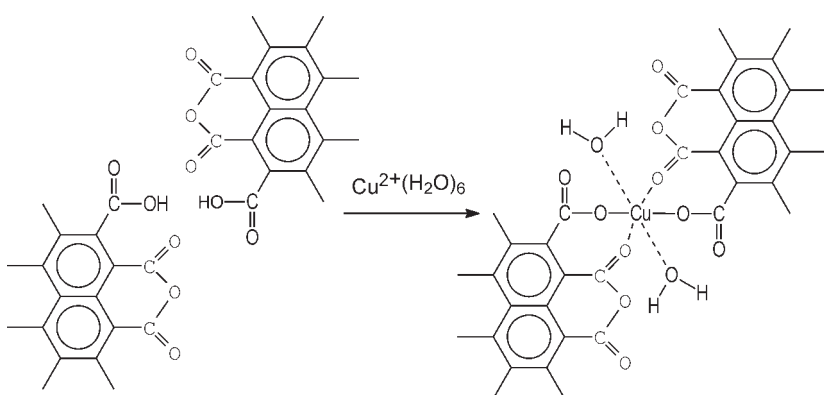


Figure 7. Postulated complexation reaction between copper(II) and carbon surface functional groups.



The metal selectivity trend remains independent of the method and extent of adsorbent oxidation, type of adsorbent precursor, porous structure, and type of adsorbent for all the materials investigated. The higher preference of adsorbents towards Cu^{2+} is a consequence of the fact that this ion often forms distorted, and hence more stable, octahedral complexes due to the asymmetric electronic structure. The generalization of metal sorptive behavior using the Irving-Williams approach leads to a novel way to understand metal sorption by active carbons and other adsorbents.

REFERENCES

1. Kadirvelu, K.; Faur-Brasquet, C.; Le Cloirec, P. Removal of Cu(II), Pb(II) and Ni(II) by adsorption onto carbon cloths. *Langmuir* **2000**, *16* (22), 8404–8409.
2. Shim, J.W.; Park, S.J.; Ryu, S.K. Effect of modification with HNO_3 and NaOH on metal adsorption by pitch-based activated carbon fibers. *Carbon* **2001**, *39* (11), 1635–1642.
3. Corapcioglu, M.O.; Huang, C.P. The adsorption of heavy metals onto hydrous activated carbon. *Water Res.* **1987**, *21* (9), 1031–1044.
4. Budinova, T.K.; Gergova, K.M.; Petrov, N.V.; Minkova, V.N. Removal of metal-ions from aqueous-solution by activated carbons obtained from different raw materials. *J. Chem. Technol. Biotechnol.* **1994**, *60* (2), 177–182.
5. Seco, A.; Mazal, P.; Gabaldon, C. Adsorption of heavy metals from aqueous solutions onto activated carbon in single Cu and Ni systems and in binary Cu–Ni, Cu–Cd and Cu–Zn systems. *J. Chem. Technol. Biotechnol.* **1997**, *68* (1), 23–30.
6. Biniak, S.; Pakula, M.; Szymanski, G.S.; Swiatkowski, A. Effect of activated carbon surface oxygen- and/or nitrogen-containing groups on adsorption of copper(II) ions from aqueous solution. *Langmuir* **1999**, *15* (18), 6117–6122.
7. Mokhosoev, M.V.; Tarkovskaya, I.A.; Krivobok, V.I.; Dubinina, M.P.; Samsonova, G.Ya.; Zharnikova, G.A. *J. Appl. Chem. USSR* **1966**, *41*, 10–14.
8. Tomashevskaya, A.N.; Tarkovskaya, I.A.; Goba, V.E.; Strazhesko, D.N. Characteristics of the sorption of metal cations by a selective cation exchanger, oxidised carbon. *Russ. J. Phys. Chem.* **1972**, *46*, 1213–1214.
9. Radovic, L.R.; Moreno-Castilla, C.; Rivera-Utrilla, J. Carbon materials as adsorbents in aqueous solutions. *Chem. Phys. Carbon* **2001**, *27*, 227–405.

10. Kuzin, I.A.; Strashko, B.K. Preparation and investigation of the ion exchange properties of oxidised coal. *J. Appl. Chem. USSR* **1966**, *39*, 566–569.
11. Strelko, V., Jr. Selective Removal of Heavy Metals Using Novel Active Carbons; Loughborough University: Loughborough, 1999; PhD Thesis.
12. Strelko, V., Jr.; Streat, M.; Strelko, V.V. Proceedings of the 23rd Biennial Conference on Carbon. 23rd Biennial Conference on Carbon, Pennsylvania State University: USA, 1997; 240.
13. Oliver, J.P.; Conklin, W.B. Proceedings of the International Symposium on the Effects of Surface Heterogeneity in Adsorption and Catalysis on Solids. Kazimierz Dolny, Poland, 1992.
14. Boehm, H.P. Some aspects of the surface-chemistry of carbon-blacks and other carbons. *Carbon* **1994**, *32* (5), 759–769.
15. Helfferich, F. Capacity. In *Ion Exchange*; Dover Publications Inc.: New York, 1995; 72–94.
16. Seki, H.; Suzuki, A. Biosorption of heavy metal ions to brown algae, *Macrocystis pyrifera*, *Kjellmaniella crassifolia*, and *Undaria pinnatifida*. *J. Colloid Interface Sci.* **1998**, *206* (1), 297–301.
17. Moreno-Castilla, C.; Lopez-Ramon, M.V.; Johns, M.M. *Carbon* **1995**, *38*, 2000.
18. Bautista-Toledo, I.; Rivera-Utrilla, J.; Ferro-Garcia, M.A.; Moreno-Castilla, C. Influence of the oxygen-surface complexes of activated carbons on the adsorption of chromium ions from aqueous-solutions—effect of sodium-chloride and humic acid. *Carbon* **1994**, *32* (1), 93–100.
19. Olivier, J.P. Modelling physical adsorption on porous and non-porous solids using density functional theory. *J. Porous Mater.* **1995**, *2* (1), 9–17.
20. Byrne, J.F.; Marsh, H. Introductory overview. In *Porosity in Carbons: Characterisation and Applications*; Patrick, J.W., Ed.; Edward Arnold: London, 1995; 1–48.
21. Jankowska, H.; Swiatkowski, A.; Choma, J. Models of adsorption and their corresponding isotherms. In *Active Carbon*; Ellis Horwood: London, 1991.
22. Gregg, S.J.; Sing, K.S.W. Physical adsorption of gases by non-porous solids. In *Adsorption, Surface Area and Porosity*; Academic Press: London, 1982.
23. Mazet, M.; Farkhani, B.; Baudu, M. Influence of heat or chemical treatment of activated carbon onto the adsorption of organic compounds. *Water Res.* **1994**, *28* (7), 1609–1617.
24. Stoeckli, H.F. Characterisation of microporous carbons by adsorption and immersion techniques. In *Porosity in Carbons*; Patrick, J.W., Ed.; Edward Arnold: London, 1995.

Interpretation of Transition Metal Sorption Behavior

1905

25. Menendez, J.A.; Illian-Gomez, M.J.; Leon y Leon, C.A.; Radovic, L.R. On the difference between the isoelectric point and the point of zero charge of carbons. *Carbon* **1995**, *33* (11), 1655–1657.
26. Kortum, G.; Vogel, W.; Andrussow, K. Tables. In *Dissociation constants of organic acids in aqueous solution*; Butterworths: London, 1961.
27. Irving, H.M.; Williams, R.J.P. The stability of transition-metal complexes. *J. Chem. Soc.* **1953**, 3192.
28. Gerloch, M.; Constable, E.C. Ligand fields, bonding and the valence shell. In *Transition Metal Chemistry*; VCH: Weinheim, 1994.
29. Winter, M.J. Consequences of d-orbital splitting. In *d-Block Chemistry*; Oxford University Press: Oxford, 1994.
30. Martell, A.E. Organic ligands. In *Stability Constants of Metal-Ion Complexes, Section II: Organic Ligands*; The Chemical Society: London, 1964.
31. Nightingale, E.R. Phenomenological theory of ion solvation, effective radii of hydrated ions. *J. Phys. Chem.* **1959**, *63*, 1381–1387.

Received August 2003

Accepted December 2003



Request Permission or Order Reprints Instantly!

Interested in copying and sharing this article? In most cases, U.S. Copyright Law requires that you get permission from the article's rightsholder before using copyrighted content.

All information and materials found in this article, including but not limited to text, trademarks, patents, logos, graphics and images (the "Materials"), are the copyrighted works and other forms of intellectual property of Marcel Dekker, Inc., or its licensors. All rights not expressly granted are reserved.

Get permission to lawfully reproduce and distribute the Materials or order reprints quickly and painlessly. Simply click on the "Request Permission/Order Reprints" link below and follow the instructions. Visit the [U.S. Copyright Office](#) for information on Fair Use limitations of U.S. copyright law. Please refer to The Association of American Publishers' (AAP) website for guidelines on [Fair Use in the Classroom](#).

The Materials are for your personal use only and cannot be reformatted, reposted, resold or distributed by electronic means or otherwise without permission from Marcel Dekker, Inc. Marcel Dekker, Inc. grants you the limited right to display the Materials only on your personal computer or personal wireless device, and to copy and download single copies of such Materials provided that any copyright, trademark or other notice appearing on such Materials is also retained by, displayed, copied or downloaded as part of the Materials and is not removed or obscured, and provided you do not edit, modify, alter or enhance the Materials. Please refer to our [Website User Agreement](#) for more details.

Request Permission/Order Reprints

Reprints of this article can also be ordered at

<http://www.dekker.com/servlet/product/DOI/101081SS120030791>